

OPEN ACCESS

Multi-Walled Carbon Nanotubes Decorated with Silver Nanoparticles for Acetone Gas Sensing at Room Temperature

To cite this article: Sheng-Joue Young *et al* 2020 *J. Electrochem. Soc.* **167** 167519

View the [article online](#) for updates and enhancements.

You may also like

- [Enhanced performance of an acetone gas sensor based on Ag-LaFeO₃ molecular imprinted polymers and carbon nanotubes composite](#)
Qian Rong, Kejin Li, Chao Wang *et al.*
- [Reactivity of inorganic nanoparticles in biological environments: insights into nanotoxicity mechanisms](#)
E Casals, E Gonzalez and V F Puentes
- [Surface plasmon resonance in gold nanoparticles: a review](#)
Vincenzo Amendola, Roberto Pilot, Marco Frasconi *et al.*



Your Lab in a Box!

The PAT-Tester-i-16: All you need for Battery Material Testing.

- ✓ All-in-One Solution with integrated Temperature Chamber!
- ✓ Cableless Connection for Battery Test Cells!
- ✓ Fully featured Multichannel Potentiostat / Galvanostat / EIS!

www.el-cell.com +49 40 79012-734 sales@el-cell.com

EL-CELL[®]
electrochemical test equipment





Multi-Walled Carbon Nanotubes Decorated with Silver Nanoparticles for Acetone Gas Sensing at Room Temperature

Sheng-Joue Young,^{1,z} Yi-Hsing Liu,² Zheng-Dong Lin,³ Kumkum Ahmed,⁴ MD Nahin Islam Shiblee,⁵ Sean Romanuik,⁶ Praveen Kumar Sekhar,^{7,*} Thomas Thundat,^{8,**} Larry Nagahara,^{9,**} Sandeep Arya,¹⁰ Rafiq Ahmed,¹¹ Hidemitsu Furukawa,⁵ and Ajit Khosla^{5,*z}

¹Department of Electronic Engineering, National United University, Miaoli 36063, Taiwan

²Institute of Microelectronics, Department of Electrical Engineering, Advanced Optoelectronic Technology Centre, Research Centre for Energy Technology and Strategy, National Cheng Kung University, Tainan 70101, Taiwan

³Department of Electronic Engineering, National Formosa University, Yunlin, Taiwan

⁴College of Engineering, Shibaura Institute of Technology, Koto City, Tokyo 135-8548, Japan

⁵Department of Mechanical Systems Engineering, Graduate School of Science and Engineering, Yamagata University, Yonezawa, Yamagata 992-8510, Japan

⁶School of Engineering Science, Faculty of Applied Science, Simon Fraser University, Burnaby, B.C V5A1S6, Canada

⁷Nanomaterials and Sensors Laboratory, School of Engineering and Computer Science, Washington State University Vancouver, Vancouver, Washington, United States of America

⁸Chemical and Biological Engineering, University of Buffalo, New York City, New York, 14260, United States of America

⁹Department of Chemical and Biomolecular Engineering, Whiting School of Engineering, Johns Hopkins University, 3400 North Charles Street, Baltimore, Maryland 21218, United States of America

¹⁰Department of Physics University of Jammu, Jammu and Kashmir 180006, India

¹¹Centre for Nanoscience and Nanotechnology, Jamia Millia Islamia, Jamia Nagar New Delhi, Delhi 110025, India

Multi-walled carbon nanotubes (MWCNTs) without and with adsorbed silver nanoparticles (Ag-NPs), are used to detect acetone vapour. MWCNTs are grown on SiO₂/Si substrates and silver (Ag) nanoparticles (NPs) are deposited onto some of these MWCNTs using electron beam evaporation method. The sensitivity of CNT based sensors (with and without NPs) increases with the concentration of acetone vapour (50 ppm to 800 ppm) while a substantial rise in sensitivity is obtained from MWCNTs with Ag NPs. Band diagrams of the MWCNTs, with and without NPs, are analyzed to understand the gas molecules adsorption phenomena. This study is the first to establish that such sensors can operate at 27 °C rather than the 180 °C–450 °C used elsewhere, thus offering significant advantages over existing methods. To investigate the sensors' dependability, they're exposed to three cycles of 50 ppm acetone gas. These tests show that the devices' responses remain unchanged, indicating their reliability. The effects of humidity upon MWCNT acetone sensors within 100 ppm of acetone vapour are also studied and improved performance towards stability and response/recovery is observed for the sensors with Ag-NPs. Furthermore, higher selectivity is observed for the Ag-coated sensors for acetone against various target gases (acetone, ethanol, NO₂, ammonia, and acetone with water).

© 2020 The Author(s). Published on behalf of The Electrochemical Society by IOP Publishing Limited. This is an open access article distributed under the terms of the Creative Commons Attribution 4.0 License (CC BY, <http://creativecommons.org/licenses/by/4.0/>), which permits unrestricted reuse of the work in any medium, provided the original work is properly cited. [DOI: 10.1149/1945-7111/abd1be]



Manuscript submitted October 16, 2020; revised manuscript received November 17, 2020. Published December 16, 2020. *This paper is part of the JES Focus Issue on IMCS 2020.*

Supplementary material for this article is available [online](#)

Gas sensors are indispensable in various environments, such as (i) industrial sensing aspects, (ii) the household and general health aspects and then (iii) diagnostics to gauge the ambient concentration of various gases. The proper identification of different volatile organic compound (VOCs) is an essential part of detecting hazardous gas leaks. Among different VOCs, acetone is an achromatic, flammable liquid, and is the smallest and simplest ketone. Acetone can be mixed with water, and as a solvent with unique properties, it is often used for cleaning in laboratories. About 6.5 million tonnes of acetone were manufactured worldwide in 2010, the main purpose of which was for its use as a solvent and for the production of methyl methacrylate and bisphenol. Acetone is harmful to human health and its concentration should not exceed beyond 250 to 1000 ppm depending on regulations set up by individual countries. For example, (i) it may cause headache, fatigue, dizziness and nausea when inhalation >500 ppm, (ii) it may cause redness, itching, irritation and eczema/chapping when skin contact >1000 ppm, (iii) it may cause nausea, stomach pain and vomiting when ingestion, (iv) it may cause eye irritation when eye contact >500 ppm.^{1–3} In organic chemistry, acetone is a common constructing unit. In

households, acetone is an active ingredient in common products as nail polish remover and paint thinner. Acetone is also created and disposed by the human body through normal metabolic processes, and can be detected in urine and blood. People with diabetes exhale relatively large amounts of acetone.⁴ Reproductive toxicity analysis show that acetone has the potential to decrease reproductive rates. Ketogenic diets that increase ketones (acetone, acetoacetic acid, and β-hydroxybutyric acid) in the blood are prescribed to infants and children with recalcitrant refractory epilepsy to counter epileptic attacks. Moreover, acetone is highly flammable and static discharges can easily burn acetone gas.⁵ Inhaling high airborne concentrations of acetone also irritates human throats. Given all of this, sensors for detecting acetone need to be investigated extensively.

Commonly, the gas sensors can be divided into four types, including catalytic combustion gas sensor, metal oxide semiconductor gas sensor, infrared gas sensor, electrochemical gas sensor. Among them, the advantages of metal oxide semiconductor gas sensor are long life and low price than other. In recent years, the various morphologies in the field of semiconductor—such as nanotubes,⁶ nanoparticles (NPs),⁷ nanobelts, and nanowires⁸—has led to improved sensitivities and response times for sensing materials with highly specific surface areas.^{9–16} The use of chemical sensors, particularly those based on the change of electrical signals after the binding of detected chemical species or gases, is a popular method for fabricating low-power, low-cost, and high-accuracy

*Electrochemical Society Member.

**Electrochemical Society Fellow.

^zE-mail: shengjoueyoung@gmail.com; khosla@yz.yamagata-u.ac.jp

portable sensing devices with unique electrical, physical, and chemical characteristics and excellent adsorption capacity for chemical materials. Several metal oxide semiconductors are widely used as active components in sensing layers. However, these materials are generally most effective as sensors only at elevated temperatures.^{17–21}

Carbon nanotubes (CNTs) have metallic or semiconducting characteristics depending on their chirality and shape, and thus may be used in a fashion that is electrically similar to metals or semiconductors.^{22,23} Sensors for chemical gases based on semiconducting CNTs, which are known to perform effectively, can be used to detect toxic gases and pollutants, such as ethanol, CO, and isopropyl alcohol.^{24–27} Generally, the gas sensor was used to metal oxide film as active layer. Although, the metal oxide-based gas sensor can detect different gases type and its sensitivity is very high. However, it is very power consumption because the work temperature of metal oxide-based gas sensor is very high (about 200 °C to 400 °C).²⁸ CNTs are often used as sensors for different gases because they have large surface areas for adsorbing gas molecules and hollow geometries that can increase sensitivity and reduce operating temperatures.²⁹ The sensing mechanisms of CNTs, which depend on the transfer of electrons from- and to- the molecules adsorbed on a material surface, may remain active even in the presence of surface-adsorbed species—in which the transfer of electrons occurs after the interaction between different analytcs.^{23,30} The literature shown that the CNTs-based gas sensor can operate at room temperature (28 °C), and it can improve gas sensing performance though adsorb noble metal NPs.^{31–35} Thus, the CNTs are promising candidates for gas sensing applications.^{31–35}

This study investigates the growth of CNTs on Si substrates and the adsorption of silver (Ag) NPs onto those surfaces. The properties of CNTs sensors, without and with adsorbed Ag NPs, that are associated with acetone vapours are comprehensively analysed and room temperature sensing performances such as sensitivity, stability, reliability, effect of humidity and selectivity are systematically studied.

Experimental

MWCNT fabrication and Ag NPs deposition.—Si (100) substrates are initially cleaned via immersion in boiled acetone for

~600 s and then in boiled isopropyl alcohol for another ~600 s.²⁰ The cleaned substrates are next rinsed in deionised water and then dried with flowing N₂ gas. The substrates are next thermally oxidised, to form a ~20 nm thick SiO₂ layer. This SiO₂ film acts as a catalyst diffusion barrier layer prior to depositing a 10 nm thick Fe layer via sputtering.^{22,36} Subsequently, the Si substrates are placed on an Al₂O₃ boat inside a tube-typed furnace in the horizontal direction. Only inert N₂ gas is injected into this Al₂O₃ tube during the upcoming CNT growth. The N₂ gas flow rate is controlled at 100 sccm, and the pressure within the tube is held at 6.5 Torr for 20 min. The temperature of this pre-treatment process is maintained at 600 °C.

Upon increasing the chamber temperature to 700 °C, the N₂ gas valve is switched off and the C₂H₂ reactant gas valve is switched on to grow the high-density multi-walled (MW-) CNTs. The C₂H₂ gas flow rate is controlled at 30 sccm, and the chamber pressure is kept at 3.5 Torr for 600 s. Next, the C₂H₂ reactant gas valve is turned off to halt CNT growth, the temperature of the tube furnace is decreased to room temperature, and the N₂ gas valve is switched off to further decrease the temperature to less than 100 °C.

To create our CNT-based acetone sensors with Ag NPs, an electron beam (E-beam) was utilized to evaporate a controlled load of noble metal Ag NPs all over the CNTs to an equivalent nominal thickness of ~15 nm. Then, a metal mask which is designed the width of 1 mm and a length of 5 mm as contact electrode, and sensing area of 25 mm². After the metal mask covered on Ag NPs CNTs, a thickness of 100 nm Ag film is deposited by thermal evaporation system. The device schematic, without and with Ag NPs, is shown in Figs. 1A, 1B and S1 (available online at stacks.iop.org/JES/167/167519/mmedia), respectively.

The surface morphology of the sample was then characterized by a Hitachi S-4700I field-emission scanning electron microscope (FESEM) that was operated at 15 keV. A Philips TECNAI 20 high-resolution transmission electron microscopy (HRTEM), operated at 200 kV, and a VG Scientific ESCA LAB 250 were used to characterize the elements and bonding in the CNT. The Raman spectrum of the CNT was also obtained using a HORIBA JOBIN YVON B299-421 system with 514 nm laser excitation.

The acetone-sensing experiments are performed using a high-vacuum I-V measurement system and a Keithley 2410 semiconductor parameter analyzer. The size of gas chamber is 10.6 dm³. The

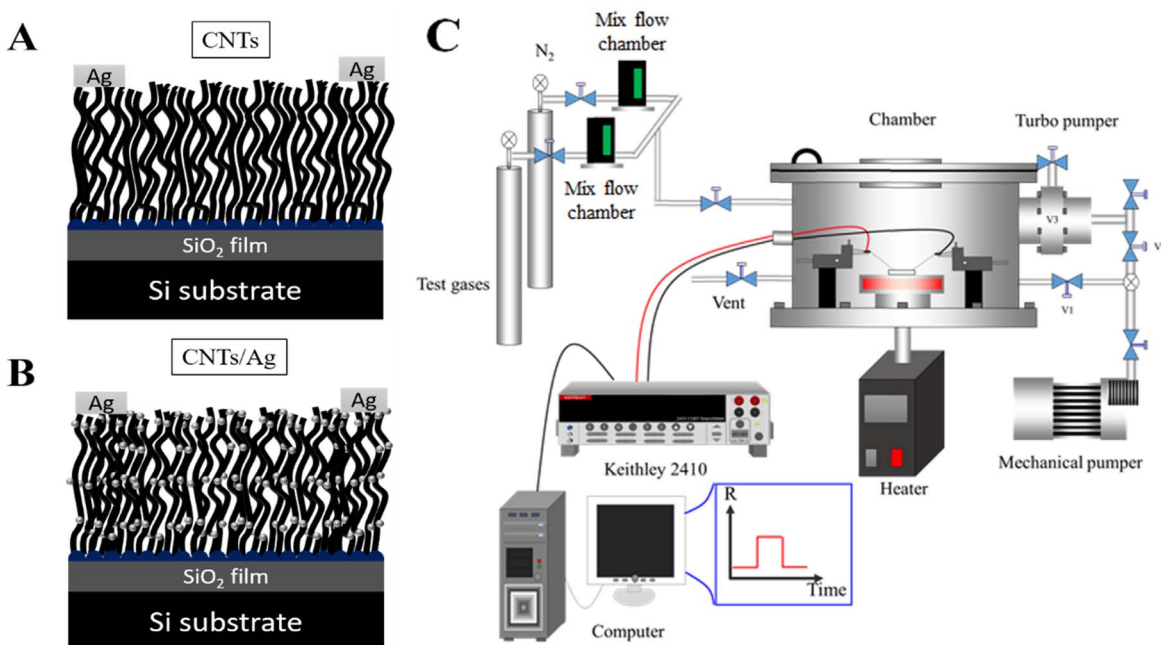


Figure 1. Schematics of sensing devices and experimental apparatus. (A) Device structure of fabricated CNT-based acetone gas sensor without adsorbed Ag NPs. (B) Device structure of fabricated CNT-based acetone gas sensor with adsorbed Ag NPs. (C) Schematic of experimental sensing apparatus.

resistance of CNTs, without and with adsorbed Ag NPs, at different acetone concentrations is measured in a series of acetone filling and pumping cycles, with filling pressures ranging from 50 to 800 ppm.²³ Figure 1C schematically depicts this experimental sensing apparatus.

Results and discussion

Characteristic analysis of Ag NPs adsorption onto MWCNTs.—

The surface morphologies of the CNTs, with and without Ag NPs, are characterised using FESEM and high-resolution (HR-) transmission electron microscopy (TEM). Figure 2A shows a cross-sectional field emission scanning electron microscopy (FESEM) image of the grown CNTs. The average length and diameter of the CNTs are $\sim 4.5 \mu\text{m}$ and $\sim 31.5 \text{ nm}$, respectively.

The adsorption of Ag NPs onto the CNT surfaces is conducted following a process similar to that previously reported.²² Specifically, the evaporation of Ag NPs with a controllable load via an electron beam (e-beam) is conducted on the CNTs, with the grown Ag NPs exhibiting an average equivalent thickness of $\sim 15 \text{ nm}$. Figure 2B presents a bright-field TEM image of a low-magnified CNT region with Ag NP adsorption, in which the Ag NPs are uniformly coated onto the CNT surfaces. Figure 2C provides a HRTEM image of part of Fig. 2B. Some Ag NPs have separated from one another on a given CNT surface, whereas others have accumulated. According to our statistical results, the average size of each Ag NP is $\sim 14.85 \text{ nm}$. The energy dispersive spectroscopy (EDS) detected C and Ag elements. The detailed information can be found in Fig. S2.

The Ag NP-decorated MWCNTs are further analysed using electron spectroscopy for chemical analysis System (ESCA). Figure 3A shows the two peaks of the resulting XPS spectrum, one with a 376.25 eV binding energy that belongs to the Ag $3d^{3/2}$ orbital and another with a 370.25 eV binding energy that belongs to the Ag $3d^{5/2}$ orbital. The doublets of ESCA spectra are indicative of Ag.³⁷ Figure 3B presents the Raman spectra of CNTs without Ag NP decoration, within which two peaks are also observed. One peak is located at 1350 cm^{-1} and belongs to the D band mode, whereas the other peak is located at 1580 cm^{-1} and belongs to the G band mode (tangential stretching mode, E_{2g}). These results indicate the presence of MWCNTs.³⁸

Sensor performance and reliability.—Figures 4A and 4B show the sensing responses of CNTs, without and with Ag NP-decorated, during different acetone filling and pumping cycles, in which the filling pressures change from 50 to 800 ppm. These measurements are taken by injecting different acetone gas concentrations into the

test chamber and the sensor is set to 5 V. Figures 4A and 4B present the sensing signals in response to acetone gas with different concentrations for our CNTs, without and with Ag NPs. The sensitivity (S) can be defined as the following equation:.

$$S = \left[\frac{R_{gas} - R_0}{R_0} \right] \times 100\%$$

where R_{gas} is the resistance of CNTs saturated with adsorbed gas in the test chamber during the acetone gas filling half-cycle and R_0 is the resistance of these same CNTs during the pumping half-cycle.²³ The resistivity, and thus the sensitivity, of the fabricated CNT sensors respond rapidly towards acetone gas being injected into- or being pumped out from- the chamber. Figure 4A shows that the response of sensors without Ag NPs to a given injected acetone gas concentration are: 0.51% at 50 ppm, 0.64% at 100 ppm, 0.85% at 200 ppm, 1.12% at 400 ppm, and 1.53% at 800 ppm. Figure 4B demonstrates that the addition of Ag NPs increases the response of such sensors to: 1.61% at 50 ppm, 1.90% at 100 ppm, 2.43% at 200 ppm, 3.00% at 400 ppm, and 3.43% at 800 ppm. These results prove that Ag NPs-decorated can improve the sensitivity of CNT-based gas sensors, and that the sensors' responses moreover increase along with acetone gas concentration. Satheshkumar et al.³⁹ also found that Ag-coated ZnO nanowire-based volatile organic compound (VOC) gas sensors possess a relatively high sensitivity. They found that the surface enhancement effect on their nanowires can be utilised for detecting VOCs using attenuated total reflectance Fourier-transform infrared (ATR-FTIR) spectroscopy. Our findings using our Ag NPs-decorated MWCNT sensing of acetone can be theoretically attributed to the as-grown CNTs being naturally p-type and to acetone being a reducing gas. Consequently, the resistance of the CNTs will increase as the sensors become exposed to acetone gas.²²

Figures 4A–4B also show that the CNTs with Ag NPs have more stable sensing characteristics than the CNTs without Ag NPs. When the acetone gas is maintained at a certain concentration for measurement: the S values of CNTs without Ag NPs increase slightly, whereas the S values of CNTs with Ag NPs are relatively constant. These results suggest that the CNTs with Ag NPs have a rapid response because they can quickly reach stable S values. Penza et al.³⁰ found that CNT-networked film gas sensors with adsorbed gold (Au) nanoclusters have a higher sensitivity than devices without such Au nanoclusters, with the difference between the two structures attributed to the capability of the Au nanoclusters to strengthen the interaction of the CNT surfaces with the exposed gas.³⁰

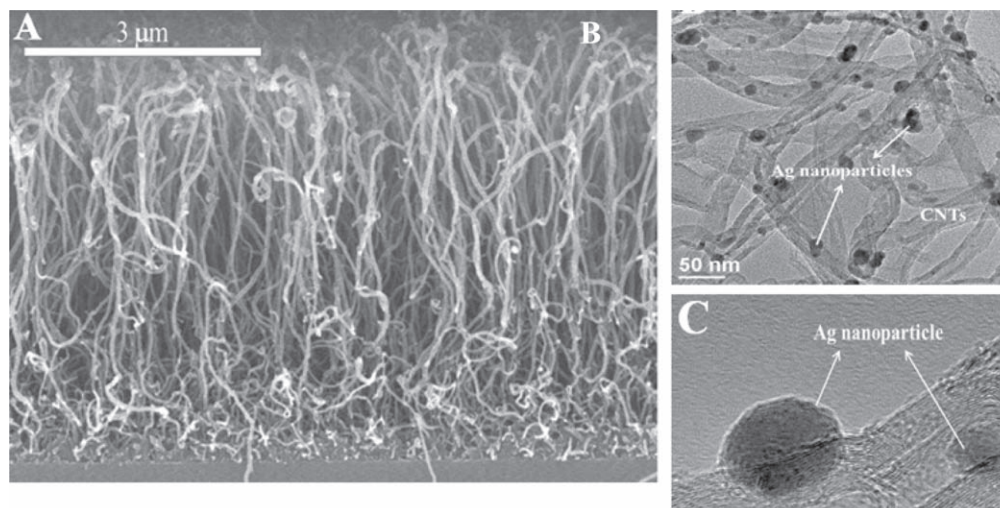


Figure 2. Microscopy images of grown CNTs and deposited Ag NPs. (A) Cross-sectional FESEM image of CNTs. (B) Low-magnification bright-field TEM image of CNTs with adsorbed Ag NPs. (C) HRTEM image of an edge-part of (B).

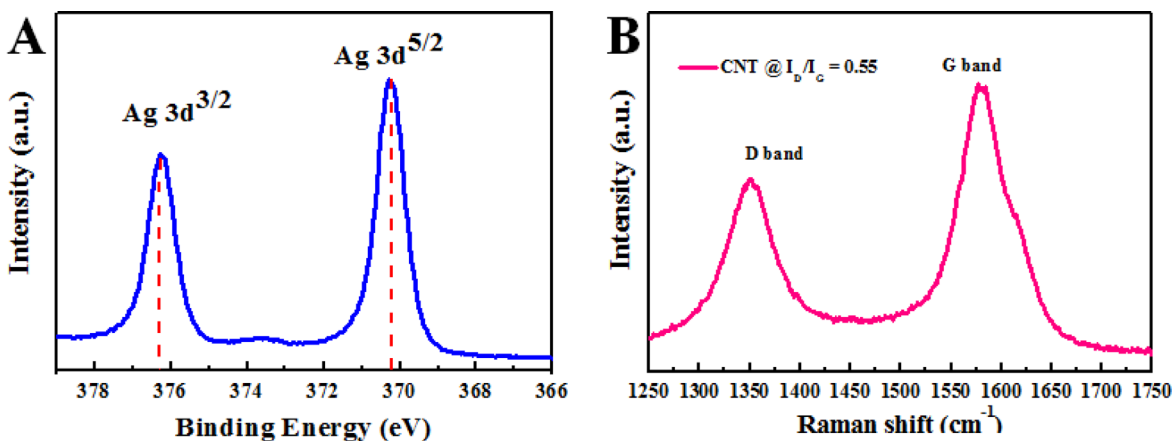


Figure 3. ESCA and Raman spectra analyses of Ag NPs and CNTs. (A) ESCA spectra of Ag NPs. (B) Raman spectrum of CNTs at room temperature.

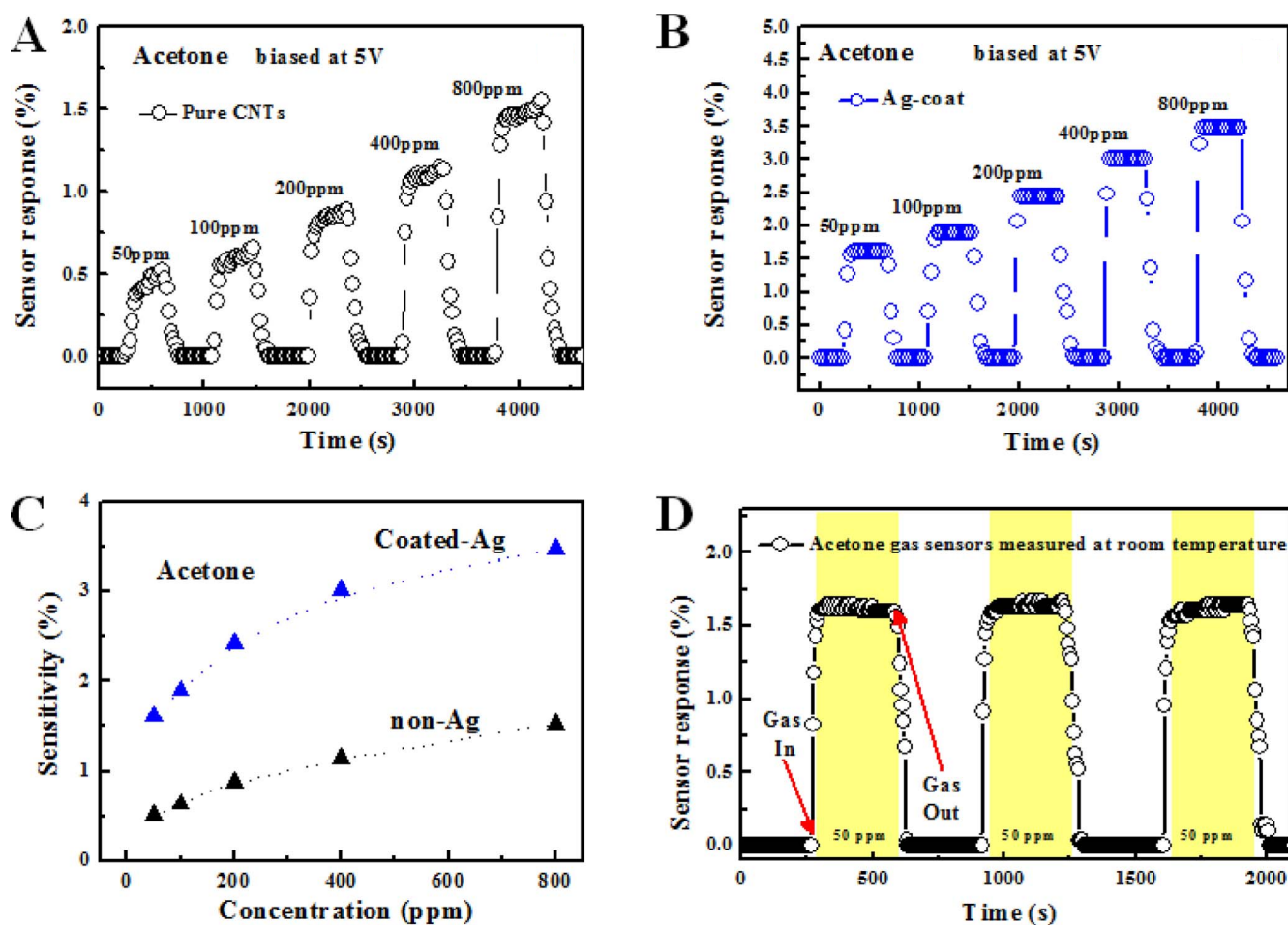


Figure 4. Sensor response and sensitivity, with and without adsorbed Ag NPs, in response to different acetone gas concentrations. (A) Sensor response, without Ag NPs, at various acetone gas concentrations. (B) Sensor response, with adsorbed Ag NPs, at the same acetone gas concentrations. (C) Sensitivities of CNT-based sensors, without and with Ag NPs, at various acetone gas concentrations. (D) Reproducibility and stability of CNT-based sensor responses, with adsorbed Ag NPs, to a 50 ppm acetone gas concentration.

Figure 4C presents the sensitivity of the MWCNT sensors, with and without Ag NPs, at different acetone gas concentrations. With or without Ag NPs, these MWCNT-sensors exhibit sensitivity to acetone gas. The Ag NP-decorated increases the response magnitude and enhances both the sensing rate and sensitivity of the devices. This enhancement of sensitivity may be caused by the graphitisation of the CNTs.⁴⁰ The five types of potential adsorption sites on the CNTs are as follows: parts of the external surfaces supplemented

with Ag NPs, external groove sites, interstitial channels, internal (endohedral) sites, and the external surfaces themselves.^{27,41,42} Subsequently, to determine the dependability of MWCNT acetone sensors with adsorbed Ag NPs, 50 ppm of acetone gas is injected into the measurement system and exposed to the sensor. The sensors are tested in three pumping cycles. As shown in Fig. 4D, the results of this reliability test indicate that the performance of the sensor response has not changed. As such, Fig. 4D suggests that the

fabricated sensors are highly reliable. Here, five CNT sensors without Ag NPs and five CNT sensors with Ag NPs are fabricated, all of which exhibit similar characteristics during testing. The standard deviations of all of the measured results are within 5%.

Gas molecules adsorption physics.—Figure 5A shows the decreasing trend of gas adsorption on the oxidised Ag surface plane. Oxygen atoms occupy standard face-centred cubic (FCC) in-plane positions on the oxidised Ag monolayer structure.⁴³ An extra negative charge is taken by the oxygen because its electronegativity is higher than that of Ag, i.e. additional transfers occur from the Ag to the oxygen atoms.⁴⁴ These oxygen ions lead to electron-depleted regions at the Ag nanocluster surfaces, providing more effective adsorption sites for gas reduction. Ag has a large electron affinity at 2.0–2.5 eV, and the reducing gas molecule will interact with the Ag atom of the active adsorption centre.⁴⁵ A net charge transfer from

one reducing gas molecule to Ag is obtained in this study. If the oxidation state of the promoter changes with the surrounding atmosphere, then the electronic state of the semiconductor will also change accordingly in the MWCNT channels via a phenomenon called electronic sensitisation.⁴⁶

Figures 5B–5D show the schematic energy band diagrams of the CNTs (i.e. NP-free) without test vapour injection, the CNTs with test vapour injection, and the CNTs with adsorbed Ag NPs surrounded by air with test vapour injection, respectively. In the case of CNTs surrounded by air (Fig. 5B), the O₂ molecules adsorb onto the MWCNT surface to generate chemisorbed oxygen species (O₂⁻ and O⁻) by capturing electrons from the conductance band. When acetone vapour is injected (Fig. 5C), the CNTs are exposed to traces of acetone gas. By reacting with the oxygen species at the CNT surfaces, the acetone gas can decrease the oxygen species concentration at the CNT surfaces to increase electron concentration,

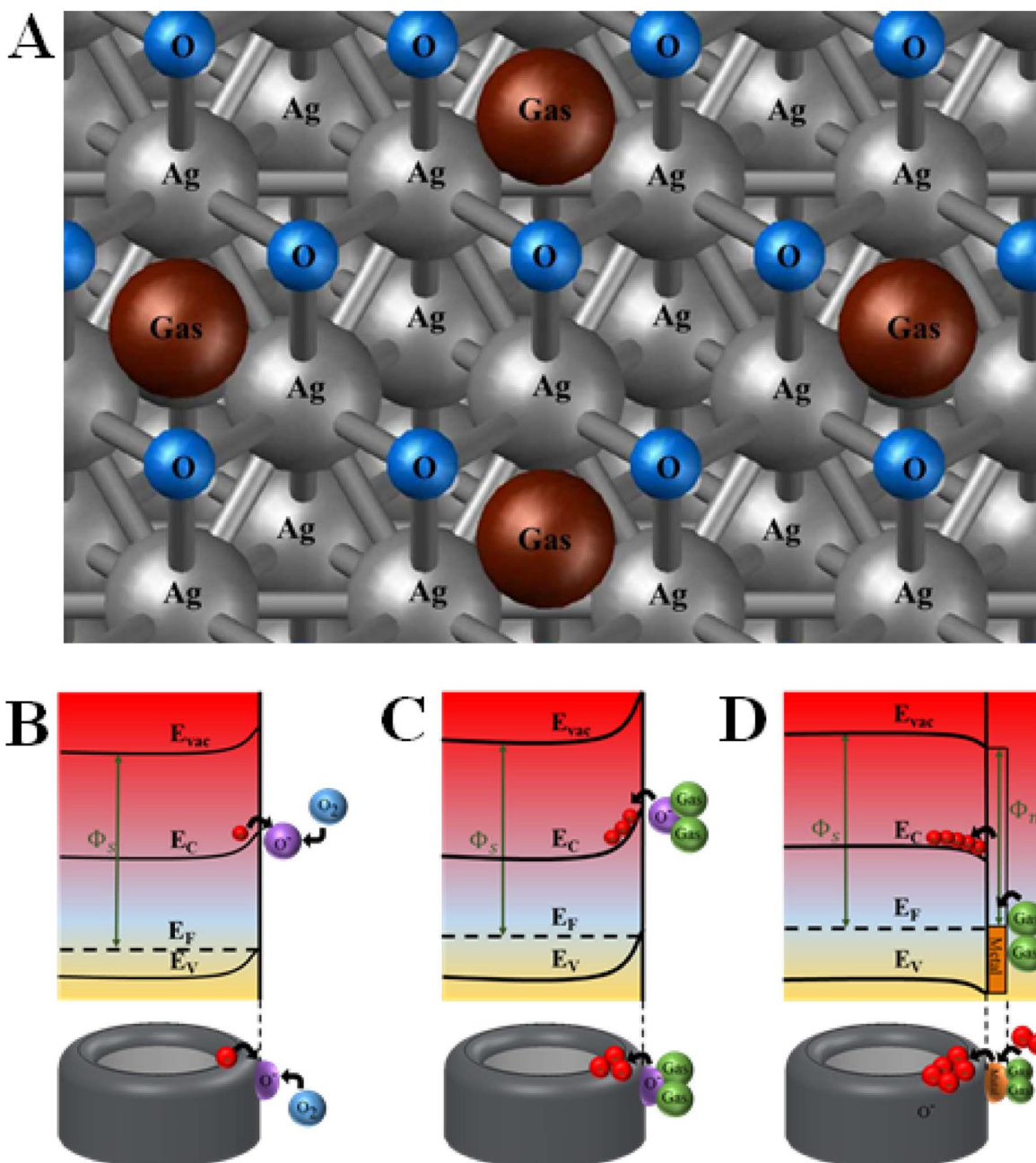


Figure 5. The physics of gas molecules adsorption by the Ag NP-decorated CNT surfaces. (A) Reducing gas adsorption on the oxidised Ag surface plane. (B) Schematic energy band diagram of pure CNTs without injected acetone gas. (C) Schematic energy band diagram of pure CNTs surrounded by air with injected acetone gas. (D) Schematic energy band diagram of Ag NP-decorated CNTs surrounded by air with injected acetone gas.

thus rendering the CNTs highly resistive. With the presence of Ag NPs on the MWCNT surfaces (Fig. 5D), O₂ molecules rapidly dissociate and generate chemisorbed oxygen species given the enhanced interaction with Ag. A substantial rise in sensitivity is thus observed for CNTs with Ag NPs. The acetone gas sensor performance of the Ag NP-decorated MWCNTs in this study increase the response magnitude and enhance both the sensing rate and sensitivity of the setup, and the values are either better than- or substantially equivalent- to those of other materials.^{17–21} Moreover, such acetone gas sensing at room temperatures is also achieved for the first time in this paper.^{17–21}

Effect of various humidity environment.—In Fig. 6A, we investigated the effect varying humidity (relative humidity (RH) = 20%, 40%, 60%, 80%, 100%) for CNTs without Ag NPs and CNTs with Ag NPs sensors with 100 ppm of acetone gas. The observed response values of pure CNTs sensors at these RH values are 0.52%, 1.26%, 2.09%, 2.97%, 4.18%, respectively. In the case of the CNTs with Ag NPs, the sensor responses at these RH values are 2.15%, 2.38%, 2.76%, 3.00%, 3.32%, respectively. The sensor response of both devices rises along with increasing humidity. This behaviour can be explained by the CNTs being p-type semiconductors in which the major charge carriers are holes in air.⁴⁶ Normally, water vapour is a reduced gas and as such water molecules can provide electrons to CNTs. When a CNTs sensor is exposed to water molecules, a charge transfer between the water molecules and the CNT occurs.

The phenomenon decreases the carrier concentration within the CNTs, thereby decreasing the conductivity of the CNT sensors. Past researchers demonstrated that humidity can influence the response of CNT-based sensors.^{47–50} In Fig. 6B, the CNTs sensor without Ag NPs response increases, ratio was higher than that of CNTs sensors with Ag NPs at the same RH. These results show that CNT sensors without Ag NPs readily respond to varying humidity. In the case of the Ag NP decorated CNT sensors, there is likely reduced cross sensitivity to water molecules, which results in an improved performance of these sensors with respect to their stability and response/recovery. In Fig. 6C, the selectivity of the gas sensing of CNTs without Ag NPs and CNTs with Ag NPs were tested against various target gases including acetone, ammonia, ethanol, NO₂, and acetone with water vapour. The observed sensor responses to acetone are higher than ammonia, ethanol, and NO₂. This data proves that CNTs with Ag NPs have excellent selectivity for acetone, and moreover the response, stability, and response/recovery of such sensors are enhanced within a more humid environment.

Conclusions

The growth of high-density MWCNTs on a SiO₂/Si substrate, the adsorption of Ag NPs onto CNT surfaces, and the fabrication of CNT-based acetone gas sensors are all investigated in this study. Furthermore, the characteristics of our CNT acetone gas sensors are measured at room temperature. The sensitivity of the device

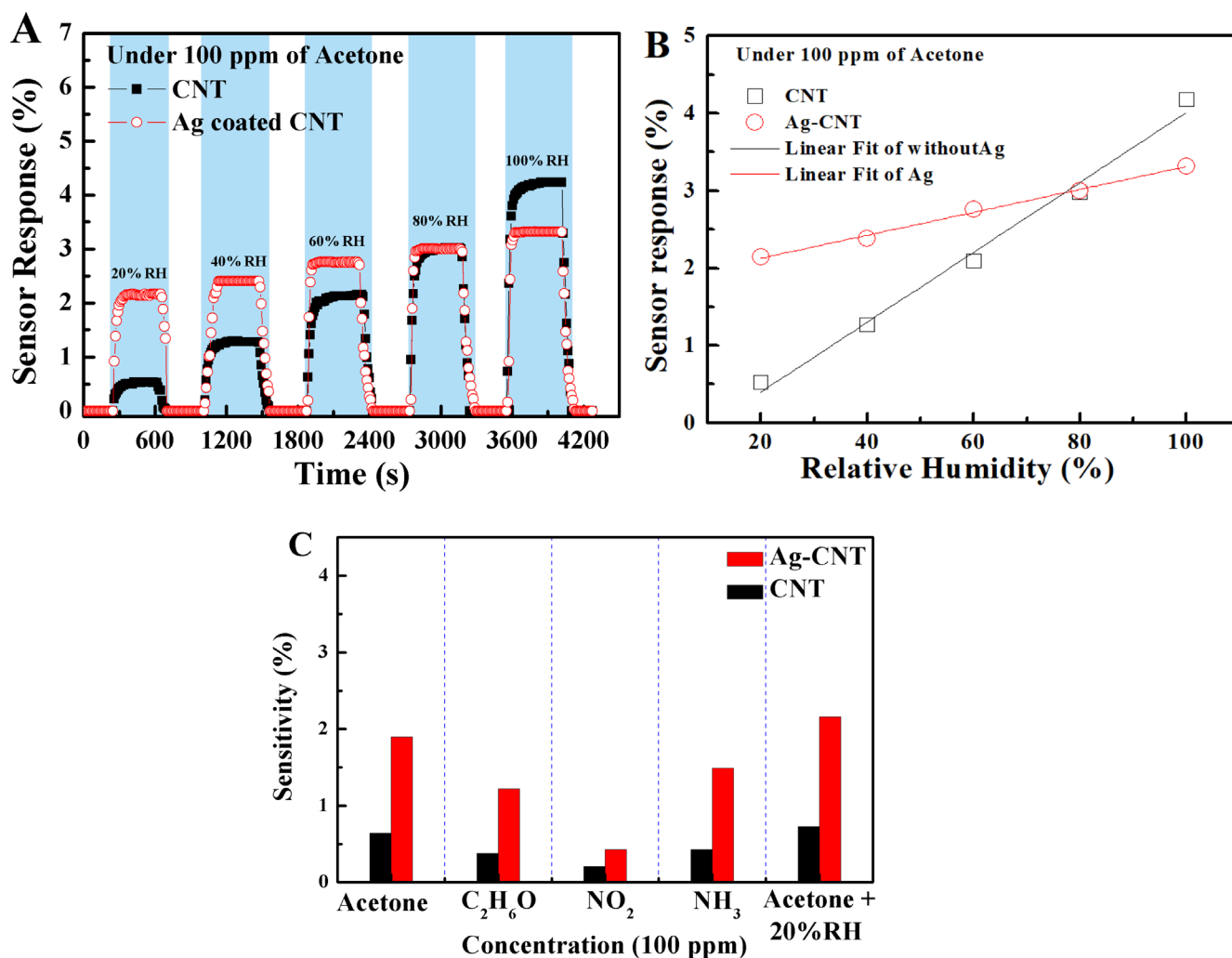


Figure 6. Effect of varying humidity for pure CNT and Ag-CNT sensors under 100 ppm of acetone. (A) Sensor response of CNTs, with and without Ag NPs, are measured at different values of relative humidity (RH). (B) Sensor response of CNT-based sensors, with and without Ag NPs, as a function of RH. (C) Selectivity of CNT sensors, with and without Ag NPs, to various target gases (acetone, ethanol, NO₂, ammonia, and acetone with water).

increased from 0.51% using CNTs without Ag NPs to 1.61% with Ag NPs, under a 50 ppm ambient acetone gas concentration. The energy band diagrams of the CNTs with and without adsorbed Ag NPs under this ambient acetone concentration are analysed. These analytical findings show that, with Ag NPs adsorbed onto the MWCNT surfaces, O₂ molecules can rapidly dissociate and generate chemisorbed oxygen species through an enhanced interaction with Ag. The results of a reliability test show that the performance of the sensor response is essentially unchanged, indicating that the fabricated sensors are reliable. Our sensors are also evaluated in response to varying humidity under 100 ppm of acetone. These results show that CNT-based acetone sensors with Ag NPs have an excellent response, stability, and response/recovery. Thus, the measured high sensor response and strong stability in this study prove that CNT-based acetone gas sensors with adsorbed Ag NPs are favourable for gas detection applications.

Acknowledgments

The authors acknowledge the assistance of the Common Laboratory for Micro/Nano Science and Technology of the National Formosa University for some of the measurement equipment used in this study, the Center for Micro/Nano Science and Technology of National Cheng Kung University for device characterisation, and Dr. C. H. Hsiao and Dr. C. S. Huang for device fabrication and equipment support. This work was supported by the Ministry of Science and Technology under contract numbers 109-2221-E-239-031-MY2, 108-2622-E-239-010-CC3, 107-2622-E-150-002-CC2, 106-2221-E-239-037-MY3, 106-2622-E-150-005-CC3, and 106-2622-E-150-017-CC2. This study was also partly supported by the following: Grant-in-Aid for Scientific Research (Category A, Project No. 17H01224) of the Japan Society for the Promotion of Science, Centre of Innovation Program of the Japan Science and Technology (JST), Strategic Innovation Creation Project of the New Energy and Industrial Technology Development Organization of Japan, and Program on Open Innovation Platform with Enterprises, Research Institute and Academia of JST.

ORCID

Sheng-Joue Young  <https://orcid.org/0000-0003-3164-2949>
 Kumkum Ahmed  <https://orcid.org/0000-0001-6509-4093>
 MD Nahin Islam Shiblee  <https://orcid.org/0000-0002-4280-3683>
 Praveen Kumar Sekhar  <https://orcid.org/0000-0002-4669-535X>
 Sandeep Arya  <https://orcid.org/0000-0001-5059-0609>
 Rafiq Ahmed  <https://orcid.org/0000-0001-6345-3507>
 Hidemitsu Furukawa  <https://orcid.org/0000-0002-0778-3330>
 Ajit Khosla  <https://orcid.org/0000-0002-2803-8532>

References

1. K. W. Nelson, J. F. Ege Jr, M. Ross, L. E. Woodman, and L. Silverman, "Sensory response to certain industrial solvent vapors." *Journal of Industrial Hygiene and Toxicology*, **25**, 282 (1943).
2. K. Nakaaki, "An experimental study on the effect of exposure to organic solvent vapor in human subjects." *Journal of Science of Labour*, **50**, 89 (1974).
3. R. B. Dick, J. V. Setzer, B. J. Taylor, and R. Shukla, *Br. J. Ind. Med.*, **46**, 111 (1989).
4. S. V. Ryabtsev, A. V. Shaposhnik, A. N. Lukin, and E. P. Domashevskaya, *Sens. Actuators B: Chem.*, **59**, 26 (1999).
5. S. J. Young and Z. D. Lin, *Microsyst. Technol.*, **24**, 3973 (2018).
6. L. K. Randeniya, P. J. Martin, A. Bendavid, and J. McDonnell, *Carbon*, **49**, 5265 (2011).
7. E. R. Leite, I. T. Weber, E. Longo, and J. A. Varela, *Adv. Mater.*, **12**, 965 (2000).
8. Z. L. Wang, *Adv. Mater.*, **15**, 432 (2003).
9. H. M. Fahad et al., *Sci. Adv.*, **3**, e1602557 (2017).
10. J. P. Giraldo et al., *Nat. Mater.*, **13**, 400 (2014).
11. N. M. Iverson et al., *Nat. Nanotechnol.*, **8**, 873 (2013).
12. J. Zhang et al., *Nat. Nanotechnol.*, **8**, 959 (2013).
13. G. Başkaya, Y. Yıldız, A. Savk, T. O. Okyay, S. Eriş, H. Sert, and F. Sen, *Biosens. Bioelectron.*, **91**, 728 (2017).
14. Z. W. Ulissi, F. Sen, X. Gong, S. Sen, N. Iverson, A. A. Boghossian, L. C. Godoy, G. N. Wogan, D. Mukhopadhyay, and M. S. Strano, *Nano Lett.*, **14**, 4887 (2014).
15. S. Sen, F. Sen, A. A. Boghossian, J. Zhang, and M. S. Strano, *J. Phys. Chem. C*, **117**, 593 (2013).
16. F. Sen, A. A. Boghossian, S. Sen, Z. W. Ulissi, J. Zhang, and M. S. Strano, *ACS Nano*, **6**, 10632 (2012).
17. Y. Chen, H. Qin, Y. Cao, H. Zhang, and J. Hu, *Sensors*, **18**, 3425 (2018).
18. E. Wongrat, N. Chanlek, C. Chueaiarrom, W. Thupthimchun, B. Samransuksamer, and S. Choojun, *Ceram. Int.*, **43**, S557 (2017).
19. I. Hayakawa, Y. Iwamoto, K. Kikuta, and S. Hirano, *Sens. Actuators B Chem.*, **62**, 55 (2000).
20. C. Dong, Q. Li, G. Chen, X. Xiao, and Y. Wang, *Sens. Actuators B Chem.*, **220**, 171 (2015).
21. S. Kim, S. Park, S. Park, and C. Lee, "Acetone sensing of Au and Pd-decorated WO₃ nanorod sensors." *Sens. Actuators B Chem.*, **209**, 180 (2015).
22. Z. D. Lin, S. J. Young, C. H. Hsiao, and S. J. Chang, *Sensors Actuators B Chem.*, **188**, 1230 (2013).
23. S. J. Young and Z. D. Lin, *Microsyst. Technol.*, **24**, 4207 (2018).
24. L. B. da Silva, S. B. Fagan, and R. Mota, *Nano Lett.*, **4**, 65 (2004).
25. R. J. Wu, Y. C. Huang, M. R. Yu, T. H. Lin, and S. L. Hung, *Sens. Actuators B*, **134**, 213 (2008).
26. W. Li, H. Jung, D. H. Nguyen, D. Kim, S. K. Hong, and H. Kim, *Sens. Actuators B*, **150**, 160 (2010).
27. Z. D. Lin, C. H. Hsiao, S. J. Young, C. S. Huang, S. J. Chang, and S. B. Wang, *IEEE Sensors J.*, **13**, 2423 (2013).
28. S. Acharyya, B. Jana, S. Nag, G. Saha, and P. K. Guha, *Sensors and Actuators B-Chemical*, **321**, 128484 (2020).
29. K. A. Joshi, M. Prouza, M. Kum, J. Wang, J. Tang, R. Haddon, W. Chen, and A. Mulchandani, *Anal. Chem.*, **78**, 331 (2006).
30. M. Penza, M. Alvisi, R. Rossi, E. Serra, R. Paolesse, A. D'Amico, and C. Di Natale, *Nanotechnol.*, **200622**, 125502 (2011).
31. H. Guerin, H. Le Poche, R. Pohle, E. Buitrago, M. Fernández-Bolanos Badía, J. Dijon, and A. M. Ionescu, *Sens. Actuators B*, **207**, 833 (2015).
32. C. Wongchoosuk, A. Wisitsoraat, A. Tuantranont, and T. Kerdkhaoen, *Sens. Actuators B*, **147**, 392 (2010).
33. R. Leghrib, A. Felten, F. Demoisson, F. Reiniers, J. J. Pireaux, and E. Llobet, *Procedia Eng.*, **5**, 385 (2010).
34. Y. Lu, C. Partridge, M. Meyyappan, and J. Li, *J. Electroanal. Chem.*, **593**, 105 (2006).
35. A. Star, V. Joshi, S. Skarupo, D. Thomas, and J.-C. P. Gabriel, *J. Phys. Chem. B*, **110**, 21014 (2006).
36. S. Hofmann, C. Ducati, R. J. Neill, S. Piscanec, A. C. Ferrari, J. Geng, R. E. Dunin-Borkowski, and J. Robertson, *J. Appl. Phys.*, **94**, 6005 (2003).
37. E. H. Espinosa, R. Lonescu, C. Bittencourt, A. Felten, R. Erni, G. Van Tendeloo, J. J. Pireaux, and E. Llobet, *Thin Solid Films*, **515**, 8322 (2007).
38. J. Y. Miao, D. W. Hwang, K. V. Narasimhulu, P. I. Lin, Y. T. Chen, S. H. Lin, and L. P. Hwang, *Carbon*, **42**, 813 (2004).
39. E. Satheshkumar and J. Yang, *RSC Adv.*, **4**, 19331 (2014).
40. X. Zhang, J. Zhang, J. Quan, N. Wang, and Y. Zhu, *Analyst*, **141**, 5527 (2016).
41. C. S. Huang, B. R. Huang, C. H. Hsiao, C. Y. Yeh, C. C. Huang, and Y. H. Jang, *Diamond Relat. Mater.*, **17**, 624 (2008).
42. S. Shrestha, W. C. Choi, W. Song, Y. T. Kwon, S. P. Shrestha, and C. Y. Park, *Carbon*, **48**, 54 (2010).
43. F. Bartolucci, R. Franchy, J. C. Barnard, and R. E. Palmer, *Phys. Rev. Lett.*, **80**, 5224 (1998).
44. V. V. Petrov, T. N. Nazarova, A. Korolev, and N. F. Kopilova, *Sens. Actuators B*, **133**, 291 (2008).
45. N. Yamazoe, *Sens. Actuators B*, **5**, 7 (1991).
46. F. Sonia, D. Giovanni, P. Stefania, G. Andrea, and S. Luigi, *Analyst*, **144**, 4100 (2019).
47. F. Rigoni et al., *Nanotechnology*, **28**, 255502 (2017).
48. M. Y. Lone, A. Kumar, N. Ansari, S. Husain, M. Zulfequar, R. C. Singh, and M. Husain, *Sensors and Actuators A-Physical*, **274**, 85 (2018).
49. S. Freddi, G. Drera, S. Pagliara, A. Goldoni, and L. Sangaletti, *Analyst*, **144**, 4100 (2019).
50. D. Jung, J. Kim, and G. S. Lee, *Sensors and Actuators A-Physical*, **223**, 11 (2014).